Eur. Phys. J. E **2**, 47–57 (2000)

THE EUROPEAN PHYSICAL JOURNAL E

EDP Sciences

Grain boundaries and the law of corresponding cones in smectics

M. Kléman[1,a] and O.D. Lavrentovich[2,b]

[1] Laboratoire de Minéralogie-Cristallographie (UMR 7590), Universités de Paris-VI & de Paris-VII, Case 115; 4 place Jussieu 75252 Paris cédex 05, France
[2] Chemical Physics Interdisciplinary Program and Liquid Crystal Institute, Kent State University, Kent, Ohio 44242, USA

Received 21 June 1999 and Received in final form 10 September 1999

Abstract. Focal Conic Domains (FCDs) in smectic phases often assemble according to a particular rule, experimentally discovered by G. Friedel, the *law of corresponding cones* (l.c.c.). This paper reports various results relating to this type of association. First we show that a l.c.c. contact between 2 focal conic domains has a vanishing energy, yielding metastable local equilibrium. Then we use some *projective properties* of conic sections to extend the celebrated Apollonian tiling, which describes a tilt grain boundary (TiGB) of vanishing disorientation $\omega = 0$ made of toric focal conic domains, to any $\omega \neq 0$ TiGB. Finally we present a realistic model of the energy of the $\omega \neq 0$ TiGB, which we compare to the energy of a TiGB split into dislocations, and to the energy of a curvature wall. This model explains why FCD tilings show macroscopic zones not filled with FCDs.

PACS. 61.30.Jf Defects in liquid crystals – 61.72.Lk Linear defects: dislocation disclinations – 61.72.Mm Grain and twin boundaries

1 Introduction

The physics of defects in smectics (lamellar phases) has crossed all the history of modern condensed matter physics from the start. The modern concept of defect was developed by G. Friedel [1], with its full attributes, *viz.* its geometrical and topological relationship with the symmetry of the medium. A striking example of his démarche is the discovery of: a) the molecular structure of nematics—he inferred from the observation of thread-like defects (disclinations) that the molecules were parallel-aligned and located at random; b) the lamellar structure of SmAs—inferred from the observation under the light microscope of large scale defects in the shape of conjugate pairs of conics. Since these remarkable insights, our knowledge of smectic textures has proceeded rather slowly, although our interest in these bizarre defects has never failed. A proof of this interest is the number of review articles published, among them Bragg's paper [2]. However, there have been few milestones, and since Friedel's paper was in French there is a widespread ignorance of his results. Some of them will be recalled below.

A focal conic domain (FCD) is the region in space of the sample which relates to a given pair of conjugate conics. In effect, in a sample where the only defects present are pairs of conjugate conics, any molecule either belongs to a given *domain* which can be ascribed to a given pair, or belongs to none. This article is devoted to the study of some typical assemblies of FCDs, which play the role of tilt grain boundaries. We recall some simple geometrical properties of an isolated FCD in the remainder of this section.

The main characteristics of the geometry of FCDs can be found in references [1–3]. The fundamental remark is that the geometry of large scale defects in SmAs is dominated by the fact that the preferred elastic distortions are such that the layers, when curved, remain parallel and at a nearest distance equal to the equilibrium repeat distance d_0; this situation results from a balance between dilation terms and curvature terms in the free energy density which will be recalled in Section 4. Instead of the material layers, let us consider their mid-surfaces L_i (which we shall also loosely term "layers"). The L_i's being parallel, their normals are straight lines, according to an elementary result of the theory of surfaces [4]. Another elementary result is that parallel surfaces have the same centers of curvature M and P at all their intersections μ with the same normal: the principal radii of curvature are the signed lengths μM and μP, and $\sigma_M = 1/\mu M$, $\sigma_P = 1/\mu P$ the principal curvatures at μ. The centers of curvature M and P describe two surfaces which are the envelopes of the normals and which are called the focal surfaces F_M and F_P of the set of parallel surfaces L_i. At the contact of a layer L_i with the focal surfaces, one of the radii of curvature vanishes (the curvature is infinite); henceforth the focal surfaces are the sets of singular points of the geometry of parallel layers, Figure 1.

[a] e-mail: kleman@lmcp.jussieu.fr
[b] e-mail: odl@lci.kent.edu

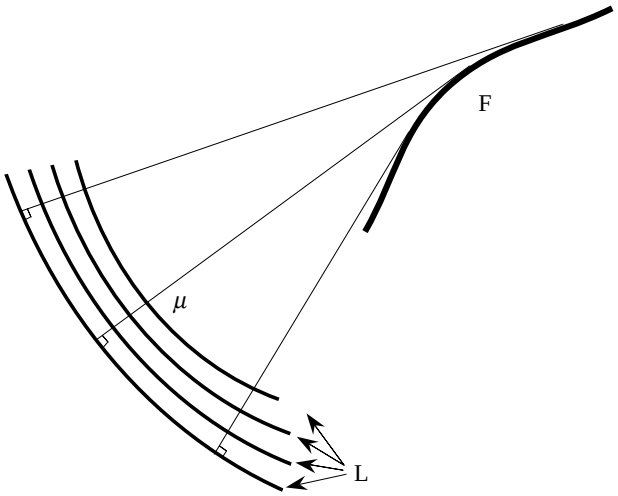

Fig. 1. Geometrical characteristics of a set of parallel surfaces (see text).

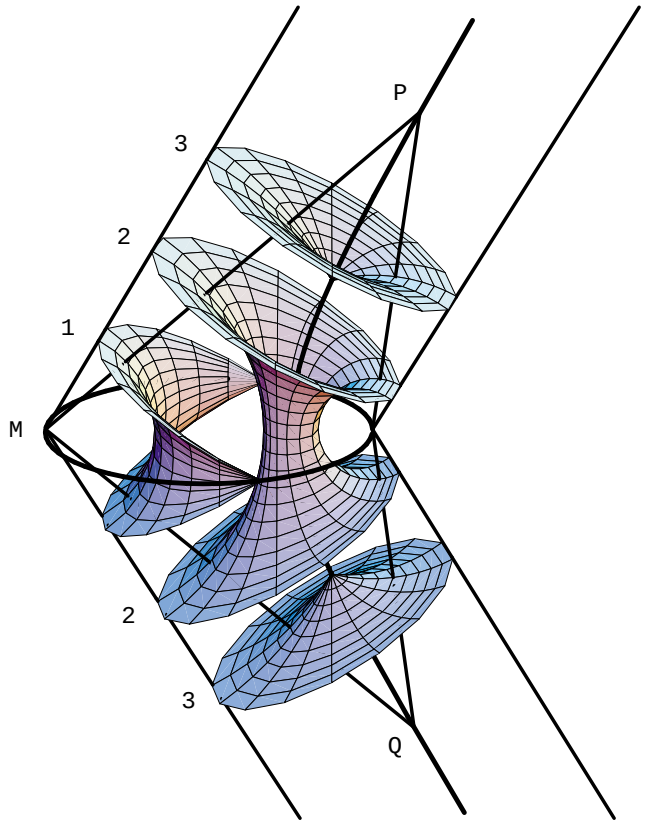

Fig. 2. Complete focal conic domain and an incomplete closed version of it, bounded by cones with vertices at points P and Q.

As a matter of fact, this situation is reminiscent of the propagation of light rays in an isotropic medium, *i.e.* one of constant index of refraction, in the approximation of geometrical optics: the light rays being the analogs of the normals to the layers, the surfaces of equal phase the analogs of the layers, and the caustics —where the light intensity diverges— the analogs of the focal surfaces — where the free energy density diverges. This is the reason why focal surfaces (2D defects) degenerate into focal lines (1D defects) in smectics of SmA and SmC type. Now a famous theorem by Dupin (see Ref. [4]) states that if the focal manifolds are both lines, these lines are necessarily a pair of *conjugate conics*, *i.e.* an ellipse and a hyperbola located in two mutually orthogonal planes, such that the foci of the ellipse (respectively, the hyperbola) are at the apices of the hyperbola (respectively, the ellipse). The layers take the shape of Dupin cyclides. In the simple case when the ellipse is a circle and (consequently) the hyperbola is a straight line orthogonal to the circle and passing through its center, the Dupin cyclides are parallel tori. A complete torus divides into two regions, one of negative Gaussian curvature and one of positive Gaussian curvature; this distinction is physically relevant —one observes experimentally either one region or the other— and extends (geometrically, physically) to more generic types of parallel Dupin cyclides. Here we consider examples with usual FCD-Is, *i.e.* FCDs whose Dupin cyclides show negative Gaussian curvature; FCD-IIs (positive Gaussian curvature [5]) will not be discussed. Figure 2 represents a *complete* FCD-I, *i.e.* the largest possible set of layers L_i of negative Gaussian curvature ascribed to a generic pair of conjugate conics. Note that M and P are the centers of curvature of all the L_i's at their intersections with the line MP.

Whatever the case, FCDs have nontrivial shapes which *do not tile space*. But since light microscopy observations indicate that FCDs assemble in large scale clusters, the question occurs, which rules do they obey when doing so, and how are the layers organized in-between, *i.e.* at the smaller scales? The case of toric FCD-Is (TFCDs: all the Dupin cyclides are parts of tori) is simple since a 2D periodic network of equal TFCDs fills space in such a way that the remaining gaps between the layers are strictly parallel and planar. The case of parabolic FCDs (PFCDs: both conics are degenerated to parabolae) has been considered experimentally and theoretically [6]; each PFCD fills all space, and the layers are practically flat at some distance from the axis of the parabolae. There is therefore a practically (but not strictly) smooth matching from one PFCD to another, as soon as the axes are parallel; such a geometry is at variance with the most generally obeyed rules of packing for generic FCDs. PFCDs are apart: they are not obtained as an analytical limit of the FCDs when the eccentricity of the ellipse tends towards $e = 1$; they will not be discussed in the following.

This paper is divided as follows. In the next section we recall (the rather old) Friedel's laws of association of FCDs, in particular the *law of corresponding cones*, whose physical meaning is elucidated (for the first time) in Section 3. In Section 4, we give closed expressions for the various contributions (singular, non-singular, topological, non-topological) which enter the *curvature energy* of a FCD. *Tilt grain boundaries* in smectics are quite often split into FCDs (Sect. 5). After having recalled the well-known power law characteristics of an Apollonian packing

of circles in Section 6, we show in Section 7 how these characteristics can be extended, by employing some *projective properties* of conics, to the case of an *Apollonian packing of ellipses* in a tilt grain boundary. Section 8 is devoted to the calculation of the *energy of a tilt boundary* split into FCDs, with *residual areas* between ellipses relaxed either by dislocations or by curvature walls. In Section 9, we compare the energy of a FCD-split boundary to the energy of a pure dislocation boundary and pure curvature walls. Scaling laws for different dislocation models are also discussed.

2 Focal conic domains of the first species and Friedel's laws of association

Usually one does not observe isolated focal conic domains in the polarizing microscope, but as already stated entire ensembles of domains in contact. These ensembles have been described in detail by G. Friedel, who has established the geometrical relations they obey [1]. We give a brief summary of these "laws", for the case of FCD-Is.

First some reminders for a unique FCD. A domain is said to be *complete* if all the layers with negative Gaussian curvature attached to a pair of *conjugate conics* have physical existence, Figure 2. A complete FCD is bounded by 2 semi-infinite cylinders of revolution which have an ellipse as a common basis, and whose generatrices are parallel to the asymptotes of the hyperbola. *Incomplete* domains can be either *closed* or *fragmented*. A closed domain is bounded by 2 *cones of revolution* which have an ellipse as a common basis, and whose vertices are on the physical branch of the hyperbola, one on each side of the plane of the ellipse usually. A well-known theorem states that the locus of the vertices of the circular cones resting on a conic is the conjugate conic; the reciprocal theorem is also true. The largest possible closed domain is obtained by taking the vertices to infinity on the asymptotes, *i.e.* it is a complete domain. A domain will be called fragmented if the ellipse is not entirely physical. It is then bounded by 2 cones of revolution whose vertices are on the ellipse. For illustrations, see reference [3].

The laws of association [1] which follow have a simple geometric content. As one will realize, they correspond physically to the tendency to fill space by insuring the *continuity of the layers* from one domain to the other, and by maintaining a *constant thickness* of the layers. Of course these requirements cannot be fulfilled everywhere, and also numerous discrepancies are observed. For example, as already stated, PFCD-Is do not stack according to these laws. But on the whole the laws allow for a correct analysis of the stacking of the layers at large scales, particularly in thermotropic specimens.

The most frequent experimental situation in thermotropic systems is that two FCDs are tangent to each other along two generatrices, and that the conics carried by these domains touch each other in pairs, *i.e.* the pairs of conics either interrupt each other or are tangent to each other. This observation due to Friedel means that the contact between two FCDs obeys the "law of corresponding cones", described below. Alternatively, if two FCDs are tangent along only one generatrix, it means that the conics they carry do not touch each other in pairs. Friedel summarizes his findings as follows.

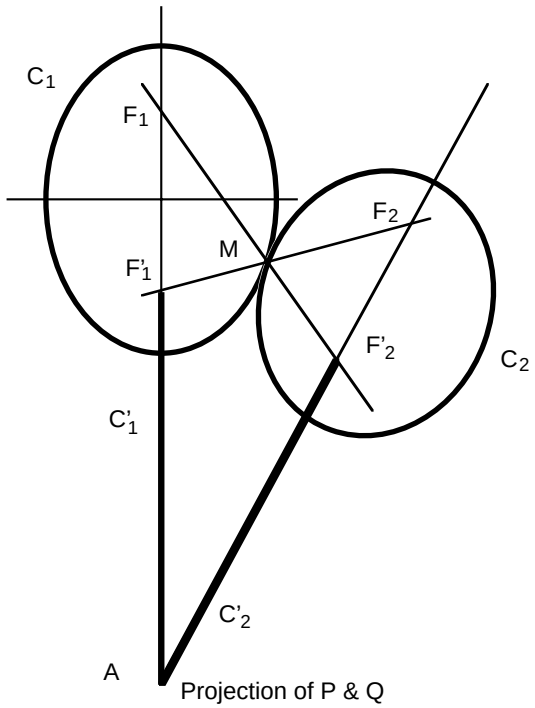

Fig. 3. Law of corresponding cones (2D view in the plane of the ellipses).

- *Law of impenetrability:* two FCDs cannot penetrate each other; if they are in tangential contact at a point M, they are tangent to each other along at least one generatrix common to two of the bounding cones.

This "law" of impenetrability is of an experimental nature; physically, its meaning is that the interactions between FCDs are of a steric nature.

- *Law of corresponding cones (l.c.c.):* when two conics C_1 and C_2 belonging to two different FCDs (FCD_1 and FCD_2) are in contact at a point M, the two cones of revolution with common vertex M, which rest on the two other conics C'_1 and C'_2 of the two FCDs, coincide. Therefore C'_1 and C'_2 have two points of intersection P and Q on the common cone, and the straight lines PM and QM are two generatrices along which the two FCDs are in contact.

This law says infinitely more than the former one; it has a physical content, discussed in the next section, and a geometrical content, which we emphasize now. If two FCDs are in contact at two points like M and P (to simplify matters, the reader may visualize C_1 and C_2 as two ellipses, and C'_1 and C'_2 as two hyperbolae, see Figures 3 and 4, but the result does not depend on such a specialization), then indeed the cones of revolution with the common vertex M and resting, respectively, on C'_1 and C'_2 are identical, because they have the same axis (the tangent to C_1 and C_2 at M), and a point in common, point

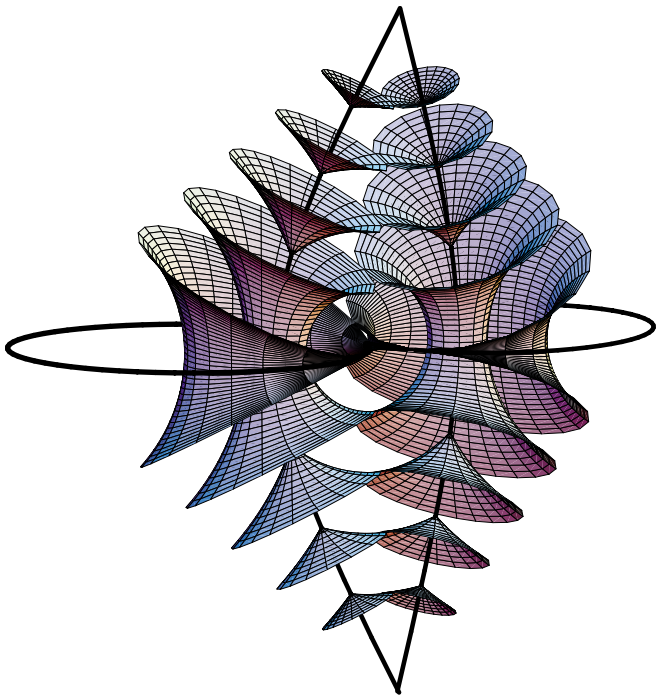

Fig. 4. Law of corresponding cones (3D view).

P. Since they coincide, C'_1 and C'_2, being on the same cone, have two intersections, P and Q. In other words, two FCDs that have one common generatrix and two contacts on their generating conics, obey l.c.c.

The law of corresponding cones leads to the geometrical construction of Figure 3. If two conics are *coplanar*, the triples F_1, M, F'_2, and F'_1, M, F_2, are aligned; F_1, F_2, F'_1, F'_2, are the foci of C_1 and C_2. Point A is the common projection of the two intersections P and Q of C'_1 and C'_2. Figure 1 of reference [7] illustrates l.c.c. in the coplanar case for a photograph by C. Williams. Figure 4 restitutes in 3D the continuity of cyclides along the generatrices of contact in the case of two incomplete FCDs obeying l.c.c.

3 Physical meaning of the law of corresponding cones

The points of contact M and P are the centers of curvature of the Dupin cyclides passing through all the points μ on the segment MP, whether they are considered to belong to one FCD or to the other. Therefore $\sigma_M \equiv \sigma_{1,M} = \sigma_{2,M}$, $\sigma_P \equiv \sigma_{1,P} = \sigma_{2,P}$, where $\sigma_M = 1/\mu M$, $\sigma_P = 1/\mu P$ are the principal curvatures at μ; μM and μP are signed lengths. The same property applies of course to all the points ν on the segment MQ. The free energy density of a lamellar phase with SmA symmetry depends on: i) the invariants built with the curvatures, ii) the invariants built with the dilation of the material layers, iii) crossed terms. More precisely, when limiting ourselves to quadratic terms, the free energy density reads

$$f = \frac{1}{2}K_1(\sigma_M + \sigma_P)^2 + \overline{K}\sigma_M\sigma_P + \frac{1}{2}B\left(\frac{d-d_0}{d_0}\right)^2, \quad (1)$$

where K_1 and $\overline{K}$ are the splay and the saddle-splay elastic constants, respectively; B is the modulus of compressibility; d is the thickness of the material layer measured along its normal.

The curvature and dilation energies are in the ratio $K/BR^2 = (\lambda/R)^2$, where λ is a microscopic length (of the order of d_0). If R, a length typical of the radius of curvature, is macroscopic, this expression tells us that the curvature energy contribution is small compared to the dilation contribution, so that the total energy is expected to be pretty small when the dilation contribution vanishes identically. This is exactly the situation which is met in the theory of FCDs, and we have all reasons to believe that the theory describes the experiments quite well since so large FCDs are observed (up to 100 μm and more). However, the region near the singular lines (in a width of the order of λ, the so-called core) requires another approach.

Therefore, neglecting the dilation term away from the core, the free energy is equal at the points of contact of the two FCDs, since the curvatures are the same; there is no special energy line attached to the line of contact, and there are no forces exerted from one FCD towards the other. The geometry of contact is metastable. This is probably the best physical justification of l.c.c.

4 Energy of a FCD-I

To go further, we need the expression of the energy f_{tot} of a complete FCD [8]; we define a FCD by the semimajor axis a and the eccentricity e of the ellipse. We have $f_{\text{tot}} = f_{\text{bulk}} + f_{\text{core}}$ with $f_{\text{bulk}} = f_{\text{topo}} + f_{\text{curv}}$, where

$$f_{\text{topo}} = -4\pi\Lambda a(1-e^2)\mathbf{K}(e^2) \quad (2a)$$

is related to the "topology": $\Lambda = 2K_1 + \overline{K}$; the minus indicates that the Gaussian curvature is negative [9];

$$f_{\text{curv}} = 4\pi K_1 a(1-e^2)\mathbf{K}(e^2)\ln\frac{2b}{r_c}, \quad (2b)$$

where $b = a(1-e^2)^{1/2}$ is the semiminor axis, and r_c the core radius. As a matter of fact, r_c should be a variable quantity along the ellipse and the hyperbola [10], but we shall assume, in order to simplify things, that it is constant ($r_c \approx \lambda = \sqrt{K_1/B}$) along the ellipse and that the core energy is equal to K_1 per unit length along the ellipse. The cusp of the Dupin cyclide on the hyperbola smoothens out as one considers cyclides further away from the plane of the ellipse; the core energy decreases accordingly and becomes vanishingly small. Therefore we take the total core energy as equal to twice the ellipse core energy:

$$f_{\text{core}} = 8aK_1\mathbf{E}(e^2). \quad (2c)$$

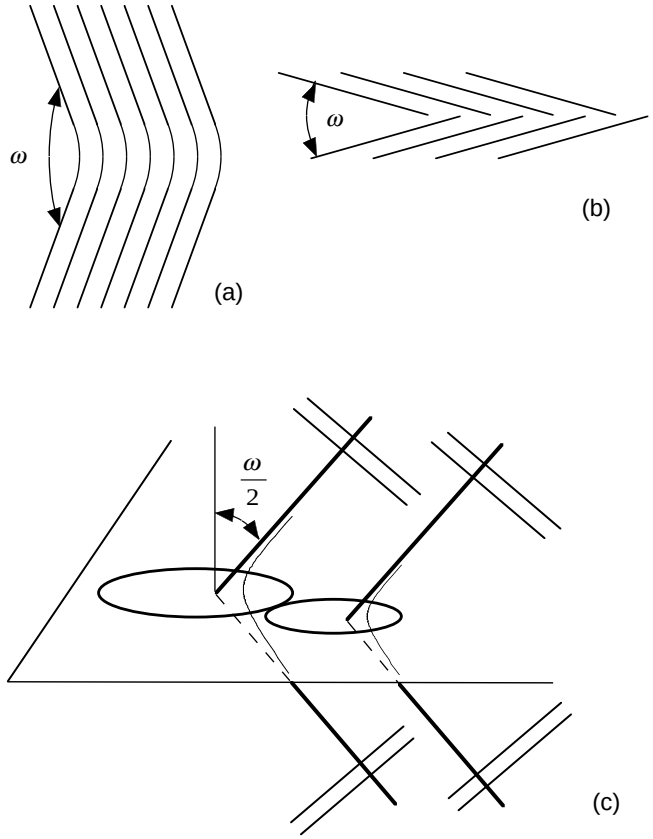

Fig. 5. Tilt grain boundary a) curvature wall; b) dislocations wall; c) FCD wall.

In the case of a TFCD ($e = 0$), the total energy scales as the radius of the focal circle.

Recall: the complete elliptic integral of the first kind is given by $\mathbf{K}(x) = \int_0^1 (1-t^2)(1-xt^2)^{-1/2}\,\mathrm{d}t$, and the complete elliptic integral of the second kind by $\mathbf{E}(x) = \int_0^1 (1-t^2)^{-1/2}(1-xt^2)^{1/2}\,\mathrm{d}t$.

5 Tilt grain boundaries split into FCDs

In smectics, tilt grain boundaries with a disorientation angle ω can be achieved according to three different geometries: curvature walls, according to a model by de Gennes [11], (Fig. 5a), dislocation walls (Fig. 5b); FCD walls (Fig. 5c). We consider here the case of FCD-split walls. The boundary is packed with ellipses of equal eccentricities $e(\omega) = \sin\frac{\omega}{2}$ and parallel long axes, and the hyperbolae have consequently parallel asymptotes. The angle between the asymptotes measures the disorientation between the two grains, since the layers are perpendicular to the asymptotic directions. The "common vertices" are at infinity on both sides and the domains are complete, Figure 6; l.c.c. is obeyed, since any pair of domains in contact at any point M on both ellipses carries the same pair of vertices P and Q at infinity.

How are the ellipses distributed in size? It is clear that in order to reduce the area of the boundary which is not occupied by the ellipses (*i.e.* which does not belong to any FCD and consequently whose energy is not curvature only) one has to introduce smaller ellipses between the larger ones, in contact with them. This "iterative filling" has to yield a minimum of the energy of the grain boundary, which requires that the *local* contacts obey Friedel's laws; on the other hand, the typical size of the non-FCD remaining interstices is fixed by a *global* energy minimization.

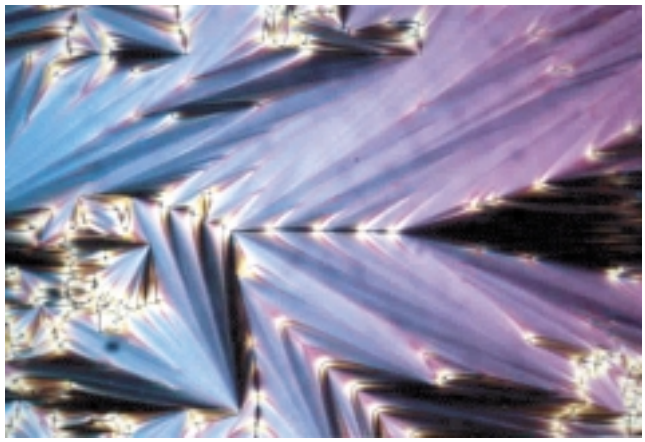

Fig. 6. Grain boundaries split into FCDs (courtesy C. Meyer). Note that the hyperbolae do not strictly meet at infinity. Therefore ω slightly varies in the GB. This is a most common case.

6 A (meta)physical grain boundary: the $\omega = 0$ Apollonian packing

This iterative filling is discussed in reference [12]. for a particular simple case of grain boundary: a boundary of vanishing disorientation $\omega = 0$. The hyperbolae degenerate to straight lines, the ellipses degenerate to circles, the FCDs are toric. TFCDs built on coplanar tangent circles trivially obey Friedel's laws. As a matter of fact, such a packing of tori is a pure representation of the mind, with little chance of physical reality, since its energy is positive, while the vanishing limit $\omega = 0$ should have vanishing energy. However, the interest is double for this case. Firstly, the consideration of the $\omega = 0$ packing puts into evidence the relationship between the *geometric parameters* of the packing and their scaling physical properties; and, as we shall see, these properties extend nicely from the $\omega = 0$ packing to a grain boundary of non-vanishing disorientation. Secondly, the $\omega = 0$ packing does *raise* correctly the question of the role of the residual areas, those regions outside the FCDs, in the energy balance, even if the solution it provides to this question has no physical reality [13]. Below we shall propose a model of the $\omega \neq 0$ grain boundary located in the smectic bulk. The *energy* of the boundary converges correctly to a vanishing energy when $\omega = 0$, because the residual areas become infinite in extent, with no inner deformation.

The *geometric* part of the $\omega = 0$ packing problem contains the two following steps: iteration of a compact packing of circles in a plane (known in mathematics as Apollonius problem; at each step of the iteration the radius of the newly introduced circles, tangent to the circles which are already present, decreases); and calculation of the size of the remaining gaps such that the global energy is minimized. The unknowns are: a) the number of circles of radius $R > b$, when the iteration reaches circles of radius b: let $g(b)$ be this number; b) the total perimeter of these circles, $P(b)$; c) the residual uncovered surface area, $\Sigma(b)$. Let L be the size of the largest circles; one expects that all the relevant quantities scale algebraically with the dimensionless quantity L/b. We can write

$$g(b) = \text{const } \left(\frac{L}{b}\right)^n; \qquad P(b) = \text{const } b\left(\frac{L}{b}\right)^n;$$
$$\Sigma(b) = \text{const } b^2\left(\frac{L}{b}\right)^n. \tag{3}$$

Numerical calculations [14] indicate that the exponent n is approximately 1.306.

The *energy* part of the $\omega = 0$ packing problem of the grain boundary is discussed in reference [12] as follows:

The energy of a TFCD of radius b scales as $K_1 b$, hence the contribution to the total energy of the circles of radius $R > b$ scales as $W_{\text{line}} \sim K_1 P(b) = \text{const } K_1 b(L/b)^n$. The residual regions are elastically deformed over a distance from the plane of the boundary of order $\lambda = \sqrt{K_1/B}$, the penetration length; hence we have $W_{\text{resid}} \sim B\lambda\Sigma(b) = \text{const } Bb^2\lambda(L/b)^n$. After minimization of $W_{\text{line}} + W_{\text{resid}}$ with respect to b, the value of b at the final iteration is $b^* \sim \sqrt{K_1/B} = \lambda$, *i.e.* a microscopic length. The energy per unit area of the grain boundary is $\sigma_{\text{FCD}} \sim L^{-2}(L/b^*)^n B\lambda^2 b^*$.

7 Generic tilt boundary $\omega \neq 0$, projective properties

Consider the set of complete FCDs carried by the Apollonius tiling. Its boundary is made of a set of parallel cylinders of revolution C tangent along common generatrices G. Cut this set by a plane Π_ω at an angle $\omega/2$ with the plane Π_0 of the Apollonius tiling. It is easy to show that the set of ellipses E_ω of eccentricity $e_\omega = \sin\omega/2$ at the intersection of Π_0 and Π_ω is a valid set of l.c.c. conics. In effect: any cone of revolution lying on an ellipse has its vertex on the conjugate hyperbola; a cylinder C lying on a circle belonging to Π_0 is such a cone; therefore the asymptotic directions are along G and the direction G_ω symmetric to G with respect to Π_ω taken as a mirror plane. The half cylinders of revolution with generatrices G and G_ω and resting on the ellipses E_ω are tangent along the same generatrices G as the set of complete FCDs carried by the Apollonius tiling for the upper half cylinders, and the mirror generatrices G_ω for the lower half cylinders. Therefore *each complete FCD of the ω-tilt grain boundary is in contact along two generatrices with its neighboring complete FCDs, Figure 7, and is in a one-to-one relationship with a complete toric domain belonging to the Apollonius filling.*

The equations (3) are modified as follows:

$$g(b) = \text{const } \left(\frac{L}{b}\right)^n;$$
$$P(b) = \text{const } \mathbf{E}\big(e^2\big)\big(1-e^2\big)^{-1/2} b\left(\frac{L}{b}\right)^n;$$
$$\Sigma(b) = \text{const } \big(1-e^2\big)^{-1/2} b^2\left(\frac{L}{b}\right)^n, \tag{4}$$

where b, the half length of the minor axis, is also the radius of the circle which projects onto the ellipse in the mapping. The perimeter of the ellipse is $4a\mathbf{E}(e^2) = 4b\mathbf{E}(e^2)/\cos\frac{\omega}{2}$; $e^2 = \sin^2\frac{\omega}{2}$; and the ratio of the areas in the mapping is $\sqrt{1-e^2} = \cos\frac{\omega}{2}$.

8 Energy of a generic tilt grain boundary split into FCDs.

The energy of a generic FCD is *not* proportional to its perimeter, according to equation (2). Let us assume for the sake of simplicity, that $\overline{K} = 0$, and that the core energy is given by equation (2c). There are 3 contributions to the total energy: the bulk energy of the FCDs, W_{bulk} (Eq. (5a)), their core energy W_{core} (Eq. (5b)), and the residual energy, W_{resid}. This last contribution depends on the model of the residual regions. There are two possible models.

$$W_{\text{bulk}} = -\int_{x=b}^{L} \mathrm{d}g(x) f_{\text{bulk}}(x)$$
$$\sim K_1 \int_b^L n\left(\frac{L}{x}\right)^n \frac{\mathrm{d}x}{x} a\big(1-e^2\big)\mathbf{K}\big(e^2\big)\left[\ln 2\frac{x}{\lambda} - 2\right] =$$
$$\alpha_b K_1 \big(1-e^2\big)^{1/2} \int_b^L n\left(\frac{L}{x}\right)^n \mathrm{d}x$$
$$\times \mathbf{K}\big(e^2\big)\left[\ln 2\frac{x}{\lambda} - 2\right]; \tag{5a}$$

$$W_{\text{core}} = -\int_{x=b}^{L} \mathrm{d}g(x) f_{\text{core}}(x)$$
$$\sim K_1 \int_b^L n\left(\frac{L}{x}\right)^n \frac{\mathrm{d}x}{x} a(x)\mathbf{E}\big(e^2\big) =$$
$$\alpha_c K_1 (1-e^2)^{-1/2}\mathbf{E}\big(e^2\big) \int_b^L n\left(\frac{L}{x}\right)^n \mathrm{d}x; \tag{5b}$$

α_b and α_c are numerical constants.

As discussed in Section 5, there are two standard models for a grain boundary, *apart from* the model under discussion, *viz.* the curvature wall model and the dislocation wall model (also called the Grandjean-Cano model). The residual regions are pieces of the grain boundaries and henceforth must adopt either a model of curvature wall or of dislocation wall. The contact between the residual regions and the wall obeys either topological (dislocation wall) or geometrical (curvature wall) relationships.

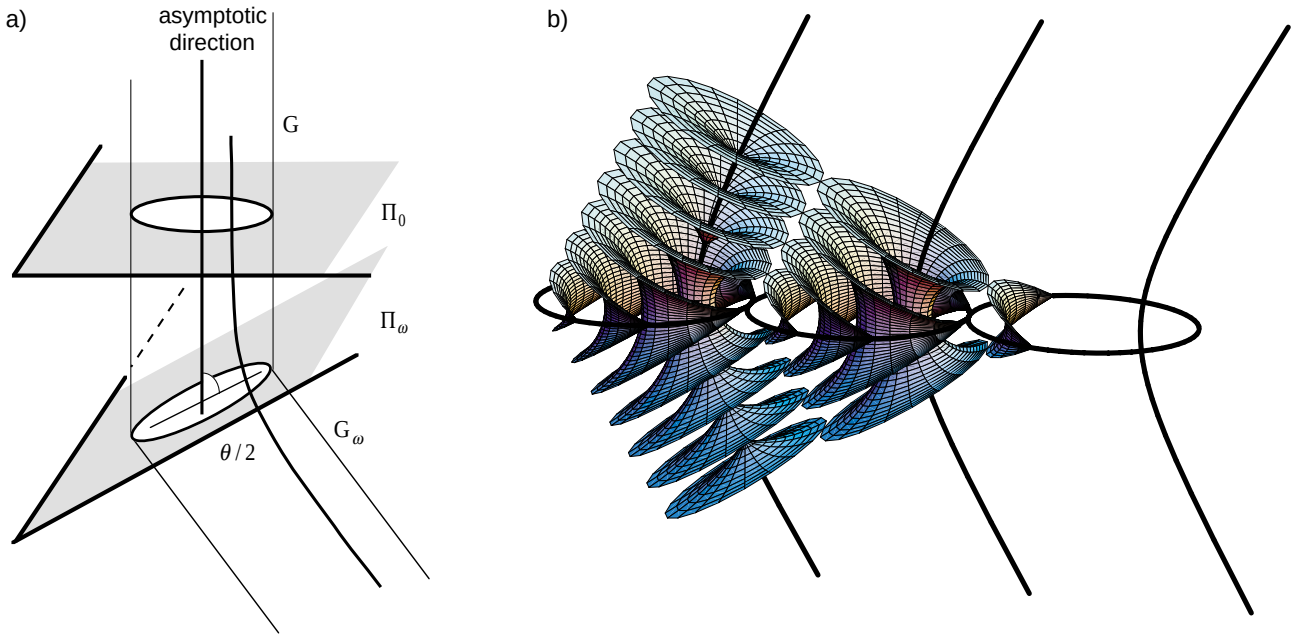

Fig. 7. Construction of a grain boundary split into FCD-Is obeying Friedel's laws of association (a); three complete FCD-Is in contact (b).

8.1 The dislocation wall model for the residual areas

According to a general analysis [15], the bending of a disclination line can be *topologically* relaxed by a wall of dislocation lines limited to the disclination. The singular lines in a FCD are disclinations (the ellipse is a disclination of half-integer strength) and are indeed bent. For small ω, it is this kind of topological relaxation which yields the most efficient energy relaxation, through edge dislocations. As shown in reference [16], the dislocations which are attached to the ellipse of an isolated FCD characterized by the quantities a and e have a total Burgers vector $b_u = 2ae$. This conservation law reflects the topological character of the relationship between the grain boundary in the residual regions, and the FCDs. In a TFCD, the circle is of zero eccentricity, $b_u = 2ae = 0$, so that there are no dislocations attached to it. The TFCD can be smoothly embedded into a system of flat and parallel layers with $\omega \equiv 0$; as already stated.

An experimental realization of ellipses and attached dislocations has been observed by polarizing light microscopy, in both thermotropic [17] and lyotropic [16] SmAs. It is directly visible that the dislocations have large, giant Burgers vectors, whose magnitude scales with the size of the ellipses, and that they are located in the plane of the ellipses. The dislocation lines have an edge character. According to standard models of dislocations in smectics, the line tension w of an edge dislocation scales as the Burgers vector [11], not as the square of the Burgers vector, *i.e.* $w \sim B\lambda ae = B\lambda be/\sqrt{1-e^2}$, if the Burgers vector is large enough. This results from the general expression for the line tension of an edge dislocation of Burgers vector b_u,

$$w = \frac{B}{2}\, b_u^2\, \frac{\lambda}{r_c} + w_c, \qquad w_c = \frac{\pi K_1}{2} \ln \frac{b_u}{2d_0} + \tau_c, \qquad (6)$$

where w_c, the core energy, contains 2 contributions: the first one relating to the curvature energy of the core region, which is split into 2 disclinations of opposite signs at a distance $b_u/2$ one to the other; the second one relating to the energy of the singular cores of the disclinations. The advantage of dislocations with large Burgers vectors is that the core energy is rather small and practically independent of the Burgers vector, since the logarithmic term varies so slowly with b_u. The core size is $b_u/2$; henceforth the principal contribution to the line tension scales as b_u. For details, see reference [11].

In the calculation which follows, we shall indeed assume that each segment of dislocation of Burgers vector $b_u = 2ae$ is extended over a region of similar size $r_c = 2a$, *i.e.* that the Burgers vector is large, scaling with the size of the ellipse to which it is attached. We have to calculate the total length of such dislocations, which we do as follows. The area of each connected residual element, at stage "b" of the iterative filling, between FCDs, scales as $\sim ab$. One can convince oneself of this scaling relation by considering four equal (a, e) ellipses in symmetrical contact two by two; they enclose a "residual" area equal to $(4-\pi)ab$. Therefore the number of connected residual elements scales as $\sim \Sigma(b)/ab = (1-e^2)^{-1/2} b^2 (L/b)^n/ab = (L/b)^n$. The length of a segment of dislocation in a connected element scales as $\sim b$. Hence the total residual energy

$$W_{\rm resid}^{\rm disl} \sim eB\lambda\Sigma(b) = Bb^2\lambda e\big(1-e^2\big)^{-1/2}\left(\frac{L}{b}\right)^n. \qquad (7)$$

Note that this expression yields a vanishing $W_{\rm resid}$ for $\omega = 0$, as expected in a realistic model.

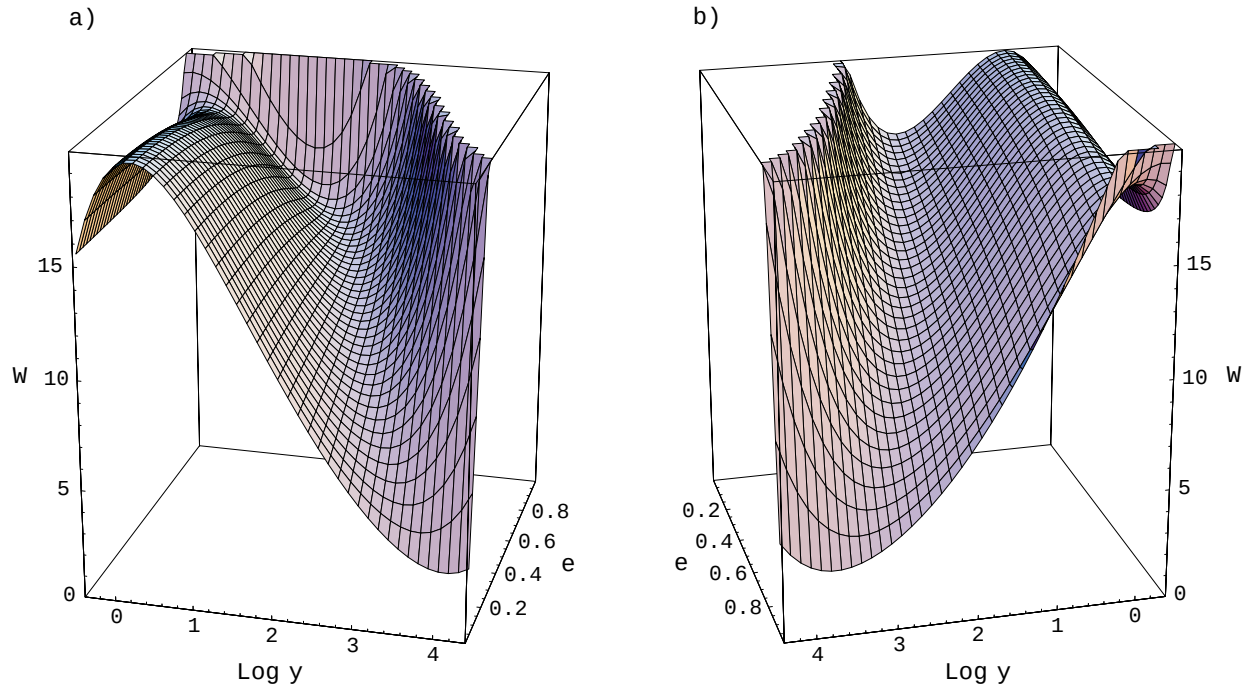

Fig. 8. Elastic energy W (arbitrary units) *vs.* e and $\log_{10} y$ for the FCD-split boundary. The residual areas are relaxed either by dislocations (a) or by curvature walls (b). In both cases, $\alpha_b = 4\pi$, $\alpha_c = 8$, $L = 50\,\mu$m, and $\lambda = 2\,$nm.

Now minimizing the total energy $W = W_{\rm bulk} + W_{\rm core} + W_{\rm resid}^{\rm disl}$ with respect to b, one gets for the minimal b

$$\frac{b^*_{\rm disl}}{\lambda} \sim \frac{1}{e}\frac{n}{2-n}\left\{\alpha_b\big(1-e^2\big)\mathbf{K}\big(e^2\big)\left[\ln\frac{2b^*_{\rm disl}}{\lambda} - 2\right] + \alpha_{\rm c}\mathbf{E}\big(e^2\big)\right\}, \tag{8a}$$

and for the energy per unit area of wall (with dislocation-relaxed residual areas):

$$\sigma^{\rm disl}_{\rm FCD}(e) \sim \frac{1}{(n-1)L^2}\left(\frac{L}{\lambda}\right)^n B\lambda^3\left(\frac{\lambda}{b^*_{\rm disl}}\right)^{n-1}\big(1-e^2\big)^{-1/2} \times\left[e\frac{b^*_{\rm disl}}{\lambda} + \alpha_b\frac{n}{n-1}\big(1-e^2\big)\mathbf{K}\big(e^2\big)\right], \tag{9a}$$

which is obtained from the integration of equations (5a), (5b), and the insertion of equation (8a) in the sum W. The value of $b^*_{\rm disl}$ for $\omega = 0$ is infinite, and the energy vanishes, as expected.

It is interesting to notice that the same qualitative results are obtained even if the dislocations which fill the residual areas are of small Burgers vector, equal to d_0, say, provided the line tension keeps proportional to the Burgers vector (not the square of the Burgers vector): $w \sim Bd_0\lambda$. The number of dislocations in a connected element area of size b is $2ae/d_0$, and the total length $\sim 2bae/d_0$. Therefore, the energy of the residual regions scales as in equation (7). In the next sections we discuss the relevance of such a model to the filling of the residual regions.

In Figure 8a, we have plotted the energy $W = W_{\rm bulk} + W_{\rm core} + W_{\rm resid}^{\rm disl}$ as a function of the eccentricity e and the dimensionless variable $y = b/\lambda$, using $\alpha_b = 4\pi$ and $\alpha_c = 8$. It is visible that for each value of e (*i.e.* of the disorientation ω) there are 2 solutions in b/λ which make the derivative vanish. The solution with the smaller, microscopic b/λ is a maximum, while the other one is a minimum. This is the valid solution; it varies rather quickly with e (or ω). The residual area is large for small disorientations ω, and the energy is small; at $\omega = 0$, the "residual" area invades the whole boundary. It is only for very large disorientations that the residual area becomes microscopic.

8.2 The curvature wall model for the residual areas

At large disorientations, the residual areas are relaxed by curvature walls. It is visible in Figure 1 that the layers of a complete FCD can be geometrically prolongated outside the FCD by two sets of parallel planar layers, perpendicular to the generatrices (*i.e.* to the asymptotic directions of the FCD) and limited to the grain boundary. Each of these layers is tangent to a Dupin cyclide all along the circle of contact, so that we expect that the physical realization of this particular geometry would not be too costly. In fact, the energy cost has two origins: the curvature walls in the residual regions (the layers do not abut abruptly on the grain boundary), and a mismatch in curvatures of the Dupin cyclides and the layers outside the FCD-Is. The first contribution can be calculated in the same way as $W_{\rm resid}^{\rm disl}$ in equation (7); it reads:

$$W_{\rm resid}^{\rm curv} \sim 2Bb^2\lambda\left[1 - \frac{e\arccos e}{\sqrt{1-e^2}}\right]\left(\frac{L}{b}\right)^n. \tag{10}$$

Here we have used the following exact expression for the curvature wall energy [18], valid for all angles:

$$\sigma_{\rm curv} = 2B\lambda\left(\tan\frac{\theta}{2} - \frac{\theta}{2}\right)\cos\frac{\theta}{2}, \qquad (11)$$

where $\theta = \pi - \omega$. The second contribution comes from the fact that the l.c.c. is not satisfied at the contact. The principal curvatures of the FCD on the circle of contact are zero and $1/R$, where R is the distance to the ellipse measured along the generatrix; the same point on the prolongating planar layer has zero curvatures. Hence the Gaussian curvatures $\sigma_1\sigma_2 = 0$ are the same but not the mean curvatures $\sigma_1 + \sigma_2$. Therefore we expect, on dimensional grounds, a surface energy density of the order of $K/R = B\lambda^2/R$, which does not depend on the parameters of the FCD. Summing over along one generatrix yields $2B\lambda^2 \int {\rm d}R/R \approx 2B\lambda^2 \ln a/r_{\rm c}$. This has to be multiplied by the total perimeter $P(b)$ in order to get an estimation of the total energy of contact, which is

$$\widehat{W} \sim 2Bb\lambda^2 \mathbf{E}\big(e^2\big)\big(1-e^2\big)^{-1/2}\left(\frac{L}{b}\right)^n. \qquad (12)$$

It is evident that $\widehat{W} \ll W^{\rm curv}_{\rm resid}$, so that, in order to compare the two models for the residual areas, it is enough, as the first step, to compare $W^{\rm curv}_{\rm resid}$ and $W^{\rm disl}_{\rm resid}$. A numerical calculation of their ratio $2[\sqrt{e^{-2}-1} - \arccos e]$ shows that the dislocation model is favoured at small eccentricities, $e < 0.4$. For $e \approx 0.4$ the two models have contributions of the same order of magnitude. The curvature wall model of the residual areas is favoured when $e > 0.4$.

Proceeding as in the previous Section 8.1, *i.e.* minimizing the total energy $W = W_{\rm bulk} + W_{\rm core} + W^{\rm curv}_{\rm resid}$ with respect to b, one gets the minimal b,

$$\frac{b^*_{\rm curv}}{\lambda} \sim \frac{1}{2\big(\sqrt{1-e^2} - e\arccos e\big)} \times \frac{n}{2-n}\left\{\alpha_b\big(1-e^2\big)\mathbf{K}\big(e^2\big)\left[\ln\frac{2b^*_{\rm curv}}{\lambda} - 2\right] + \alpha_c \mathbf{E}\big(e^2\big)\right\}, \qquad (8b)$$

and the energy per unit area of the FCD-split wall in which the residual areas are relaxed by layers' curvatures:

$$\sigma^{\rm curv}_{\rm FCD}(e) \sim \frac{1}{(n-1)L^2}\left(\frac{L}{\lambda}\right)^n B\lambda^3\left(\frac{\lambda}{b^*_{\rm curv}}\right)^{n-1} \times \left[\frac{2b^*_{\rm curv}}{\lambda}\left(1 - \frac{e\arccos e}{\sqrt{1-e^2}}\right) + \alpha_b \frac{n}{n-1}\sqrt{1-e^2}\mathbf{K}(e^2)\right]. \qquad (9b)$$

The dependence W on the eccentricity and the ratio b/λ in Figure 8b clearly reveals that the residual areas are of macroscopic size. Comparing parts (a) and (b) of Figure 8, one sees that the dislocation and curvature models of the residual areas in the FCD-split grain boundary are complementary, the first being favourable at smaller e and the second at larger e.

9 Discussion

9.1 Comparison between different models for a tilt boundary

At small disorientation, the pure dislocation model, which is observed in Grandjean-Cano wedges, has an energy per unit area of the order of $\sigma_{\rm disl} \approx B\lambda e$, practically independent of the Burgers vector (assumed small) of the dislocations. Comparing to $\sigma^{\rm disl}_{\rm FCD} \approx \frac{B\lambda^3}{L^2}\left(\frac{L}{\lambda}\right)^n\left(\frac{\lambda}{b^*}\right)^{n-1}$, where $\frac{\lambda}{b^*} \sim e$ (see Eq. (8a)), one gets:

$$\frac{\sigma_{\rm disl}}{\sigma^{\rm disl}_{\rm FCD}} \sim \left(\frac{L}{\lambda}\right)^{2-n} e^{2-n}. \qquad (13)$$

Except for very large samples, the pure dislocation model is favoured for small e.

On the other hand, at large disorientations ω (or small $\theta = \pi - \omega$), one has to compare the energy of the pure curvature wall $\sigma_{\rm curv} \approx B\lambda\theta^3 \approx B\lambda(1-e^2)^{3/2}$ to the energy of the FCD-split boundary $\sigma^{\rm curv}_{\rm FCD} \approx \frac{B\lambda^3}{L^2}\left(\frac{L}{\lambda}\right)^n\left(\frac{\lambda}{b^*}\right)^{n-1}\frac{1}{\theta}$, with $\frac{b^*}{\lambda} \to \frac{12\alpha_c n}{(2-n)\theta^3}$, equation (8b):

$$\frac{\sigma_{\rm curv}}{\sigma^{\rm curv}_{\rm FCD}} \sim \left(\frac{L}{\lambda}\right)^{2-n}\theta^{7-3n}. \qquad (14)$$

Except for very large samples, the curvature model is favoured for large e.

The FCD model should therefore be favoured for intermediate disorientations. As demonstrated in the former section, the residual areas are of the dislocation type for small eccentricities, and of the curvature type for large eccentricities. It is also a well-known experimental feature of FCD split-grain boundaries that the residual areas are of macroscopic (micron) sizes, in agreement with the present model.

9.2 Different scaling laws for the residual energy in different dislocation models

For the dislocation model, all the results and analysis rest on expression (7) for the residual energy, which assumes that the dislocation line energy scales as the Burgers vector, *i.e.* ultimately as $Bb\lambda$. The results are very different if one assumes another scaling law:

- $w \sim Bb^2$: in this case it is found numerically that the favoured residual sizes are microscopic, typically in a range $10 < b/\lambda < 100$, from small to large disorientations.
- $w \sim B\lambda^2$: in this case it is found numerically that the favoured residual sizes are giant, whatever the value of the disorientation.

This last result certainly makes the $B\lambda^2$ scaling inconsistent. But the Bb^2 scaling seems plausible; it could correspond to the filling of the residual areas by dislocations whose core is not dissociated into 2 disclinations,

but is a region where the smectic order parameter varies over a distance r_c and eventually possibly vanishes at some point. Only a detailed calculation of the Ginzburg-Landau type could give us a clue to the variation of r_c with b. It is indeed most probable that r_c varies little with b and is of the order of a coherence length [19]. A detailed calculation of the line tension of an edge dislocation of small Burgers vector yields (see Ref. [11]) $w \sim Bb^2\lambda/r_c + w_c$, where the core energy w_c would also be an outcome of the same type of calculation, and would most probably be found to be of the order of $Bb^2\lambda/r_c$. The present discussion indicates that such dislocations would have a small Burgers vector.

Note that it is not necessary that the Burgers vector be exceedingly large for a dislocation to behave as a large Burgers vector dislocation, *i.e.* to split into two disclinations. Equation (6) makes sense as soon as $b_u/2d_0$ is of the order of a few units. Large Burgers vector dislocations are such that the main contribution to the energy in the core region is curvature energy; contrariwise it is dilation energy for small Burgers vector dislocations. We therefore expect that the discriminating material constant between the two types of behavior is the ratio λ/d_0; this will be larger than unity for small Burgers vectors, and smaller than unity for large Burgers vectors.

Note also that in the two more "realistic" cases the qualitative results reported here are only slightly dependent on the values of the coefficients α_b and α_c.

9.3 Why an Apollonian tiling

Another implicit assumption of the model is the existence of an Apollonian tiling, *i.e.* a compact packing with tiles of different sizes, not fixed in advance, and with no entropy of mixing, since an iterative filling obeys quasi deterministic rules (see also Ref. [20] for a comparison between scaled and entropic tilings). The smaller conics are certainly those which would contribute more to the entropy. Now, such objects are not present in the model developed here (in the $Bb\lambda$ scaling). This remark might be a strong indication of the physical reality of the Apollonian tiling.

9.4 A caveat

Finally, a comment about the projective properties of the FCD grain boundaries. It must be understood that the successful use of these properties does not imply that there are projective invariants of physical significance in the grain boundary problem. It is only the "source" and "target" ellipses which are conserved in the projection, but there is no projective relationship between the "source" and "target" hyperbolae. All this geometry, in essence, boils down to the beautiful properties of the law of corresponding cones.

10 Conclusion

Friedel's law of corresponding cones has led us to the model of the tilt grain boundary split into FCD-Is. The elliptical bases of FCD-Is lie in the plane of the boundary; the disorientation angle ω coincides with the angle between asymptotic directions of the hyperbolae on both sides of the boundary and determines the eccentricity e of the ellipses, $e = \sin\frac{\omega}{2}$. The packing of ellipses follows iterative Apollonian tiling, with smaller FCD-Is inserted between larger ones. However, the iterative filling does not extend to the molecular level: the residual FCD-free areas are of macroscopic size. Depending on the disorientation angle, these residual areas are relaxed either by dislocations (small ω's) or by curvature walls (large ω's). In the limit of vanishing disorientation, $\omega \to 0$, the residual areas become infinitely large and the grain boundary degenerates into the pure dislocation wall. In the opposite limit of the largest disorientations, $\omega \to \pi$, the FCD-split boundary degenerates into the pure curvature wall with no FCDs.

The model is presented here for a SmA type of lamellar system. However, its basic features are expected to remain valid for other phases, *e.g.*, SmC liquid crystals. For example, chevron walls in both SmC and SmA samples are often seen as FCD-split boundaries [21,22]. Formation of chevrons is controlled by surface anchoring at the plates bounding the liquid-crystal slab; depending on the concrete geometry, the analysis of the FCD-split boundary above might require additional consideration of surface anchoring energies. In the SmC phase the tilt of the molecules within the smectic layers causes other complications, both topological (disclination lines in the vector field of molecular projections onto the layers [23]) and energetical (a finite energy of tilt).

We wish to thank Christophe Blanc and Claire Meyer for discussions. The work was supported by the CNRS France - NSF U.S. Cooperative Scientific Program, Grant No. INT-9726802 and by NSF STC ALCOM, Grant No. DMR89-20147.

Appendix

Dupin cyclides in this article have been drawn using Mathematica 3.0 and the following basic parameterization in Cartesian coordinates:

$$x = \frac{r(c - a\cos u\cos v) + b^2\cos u}{a - c\cos u\cos v};$$

$$y = \frac{b\sin u(a - r\cos v)}{a - c\cos u\cos v}; \qquad z = \frac{b\sin v(c\cos u - r)}{a - c\cos u\cos v},$$

where $c^2 = a^2 - b^2$, u and v are two orthogonal angular coordinates specified at the cyclides, and r is the third coordinate in direction perpendicular to the cyclides. The range of values of (u, v, r) determines whether the resulting FCD will be of positive or negative Gaussian curvature and whether it will be complete or incomplete.

References

1. G. Friedel, Ann. Phys. (Paris) **18**, 273 (1922).

2. W. Bragg, Trans. Faraday Soc. **29**, 1056 (1933).
3. Y. Bouligand, J. Phys. (Paris) **33**, 525 (1972); Y. Bouligand, J. Phys. (Paris) **38**, 1011 (1973).
4. D. Hilbert, S. Cohn-Vossen, *Geometry and the Imagination* (Chelsea Publishing Cy, New York, 1952); G. Darboux, *Théorie Générale des Surfaces* (Chelsea Publishing Cy, New York, 1954).
5. P. Boltenhagen, M. Kléman, O. Lavrentovich, C.R. Acad. Sci. Paris **315**, série II, 931 (1992).
6. C. Rosenblatt, R. Pindak, N.A. Clark, R.B. Meyer, J. Phys. (Paris) **38**, 1105 (1977).
7. J.P. Sethna, M. Kleman, Phys. Rev. A **26**, 3037 (1982).
8. M. Kleman, O.D. Lavrentovich, Phys. Rev. E **61**, 1574 (2000).
9. On the other hand, one finds that the topological energy in a domain of *positive* Gaussian curvature has to be written with the opposite sign: $f_{\rm topo}(G > 0) = +4\pi\Lambda a(1-e^2)\mathbf{K}(e^2)$. Note that $f_{\rm topo}(G > 0)$ is negative if $\Lambda = 2K_1 + \overline{K}$ is positive. $\Lambda = 2K_1 + \overline{K}$ is usually positive in a SmA phase.
10. J.-B. Fournier, Phys. Rev. E **50**, 2868 (1994).
11. M. Kléman, *Points, Lines and Walls* (Wiley, 1982).
12. R. Bidaux, N. Boccara, G. Sarma, L. de Sèze, P.G. de Gennes, O. Parodi, J. Phys. (Paris) **34**, 661 (1973).
13. The iterative geometry with $\omega = 0$ becomes physically relevant when applied to an *interface* between a lamellar and an isotropic phase rather than to a grain boundary in the bulk; at the interface, the bases of the TFCDs and the residual area differ in surface director orientation and thus bring different surface energies to the total energy balance. See: O.D. Lavrentovich, Zh. Eksp. Teor. Fiz. **91**, 1666 (1986) (Sov. Phys. JETP **64**, 984 (1987)).
14. P.B. Thomas, D. Dhar, J. Phys. A: Math. Gen. **27**, 2257 (1994).
15. J. Friedel, M. Kléman, J. Phys. (Paris) **30**, C443 (1969).
16. P. Boltenhagen, O.D. Lavrentovich, M. Kléman, J. Phys. II, **1**, 1233 (1991).
17. C. Williams, M. Kléman, J. Phys. (Paris) **36**, C1315 (1975).
18. C. Blanc, M. Kleman, Eur. Phys. J. B **10**, 53 (1999).
19. M. Kléman *The relation between core structure and physical properties*, in *Dislocations 1984*, edited by P. Vayssiére, L. Kubin, J. Castaing (Editions du CNRS, 1984). We thank one of the referees for having invited us to consider more closely the microscopic structure of the boundary itself.
20. P. Boltenhagen, M. Kléman, O.D. Lavrentovich, J. Phys. II **4**, 1439 (1994).
21. A. Fukuda, Y. Ouchi, H. Arai, H. Takano, K. Ishikawa, H. Takezoe, Liquid Crystals **5**, 1057 (1989).
22. M. Brunet, private communication.
23. L. Bourdon, M. Kléman, J. Sommeria, J. Phys. (Paris) **43**, 77 (1982).